3D geostatistical modelling for identifying sinkhole disaster potential zones around the Verkhnekamskoye potash deposit (Russia)

J J Royer[1], J Litaudon[1], L O Filippov[1], T. Lyubimova[2], N Maximovich[2]

[1]Université de Lorraine, Laboratoire GeoRessources, UMR7359 CNRS-CREGU, ENSG, 2 rue Doyen Marcel Roubault, 54505 Vandœuvre-lès-Nancy, France
[2]Perm tate University, Perm, Russia

Email: jean.jacques.royer@gmail.com

Abstract. This work results from a cooperative scientific program between the Perm State University (Russia) and the University of Lorraine (France). Its objectives are to integrate modern 3D geomodeling in order to improve sustainable mining extraction, especially for predicting and avoiding the formation of sinkholes disaster potential zones. Systematic exploration drill holes performed in the Verkhnekamskoye potash deposit (Perm region, Russia) have been used to build a comprehensive 3D model for better understanding the spatial repartition of the ore quality (geometallurgy). A precise modelling of the mineralized layers allows an estimation of the in-situ ore reserves after interpolating by kriging the potassium (K) and magnesium (Mg) contents at the node of a regular centred grid (over a million cells). Total resources in potassium vary according to the cut-off between 4.7Gt @ 16.1 % K_2O; 0.32 % $MgCl_2$ for a cut-off grade at 13.1% K_2O and 2.06 Gt @ 18.2 % K_2O; 0.32 % $MgCl_2$ at a cut-off of 16.5% K_2O. Most of reserves are located in the KPI, KPII and KPIII layers, the KPI being the richest, and KPIII the largest in terms of tonnage. A systematic study of the curvature calculated along the roof of the mineralized layers points out the location of potential main faults which play a major role in the formation of sinkhole during exploitation. A risk map is then derived from this attribute.

1. Introduction

Potassium is an alkaline element representing 2.6% of the crust's mass, and representing a crucial element for the agro-food industry which absorbs more than 90% of the world production. Potassium is used as a fertilizer for plants as it increases crop yield by 20%. Potassium stands for 15% of the world consumption of fertilizer, behind phosphate (25%) and nitrogen (60%). Due to the increase of the world demography, the FAO (Food and agriculture organization) predicts an increase in food demand of 70% by 2050, 80% of which being produced by better yields and cropping intensity. The slowdown in the arable lands expansion will stimulate further cropping intensity (multiple cropping and reduced fallow periods). Efficient and responsible use of mineral fertilizers will play a vital role in meeting future world demand for safe and nutritious food ([1], [2]). Consequently, potash production has to follow the increase of the world population for the future demand in fertilizer and for avoiding potential shortening in food production. Potassium resources are not regularly distributed worldwide as shown by the map of Figure 1. Canada, Belarus, and Russia have nearly 65% of all global reserves (Figure 2).

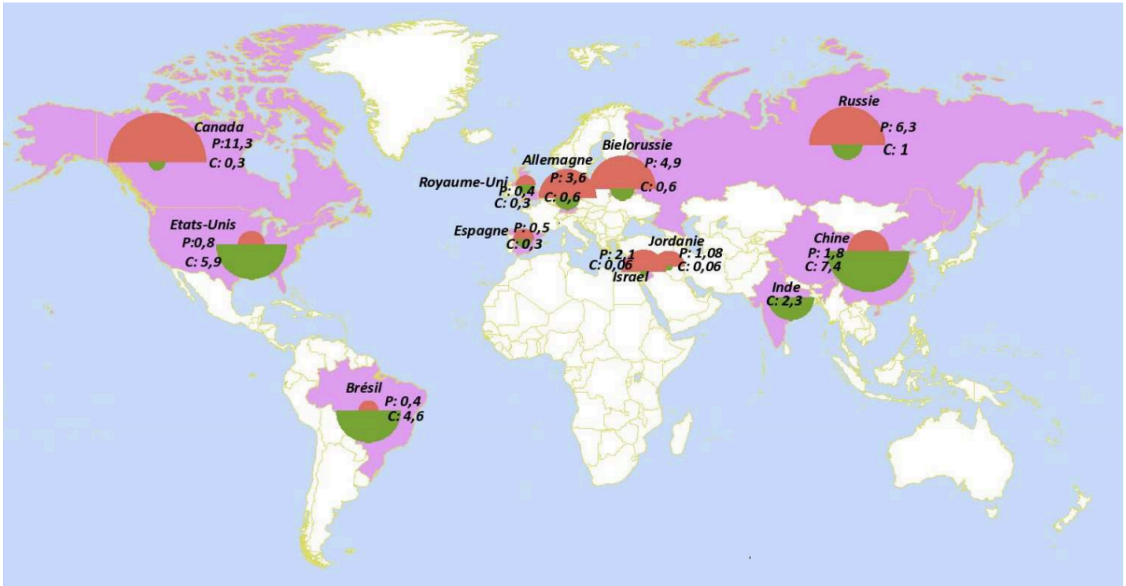

Figure 1. World potash reserves and production in Mt (Source: [1]).

Table 1 – Mineral resource estimations in sylvinite at Uralkali on 1st January 2015 (after [3])

	Category A			Category B			Category C_1			Category C_2			A+B+C_1		
Mine	**Ore (Mt)**	**K_2O (%)**	**K_2O (Mt)**	**Ore (Mt)**	**K_2O (%)**	**K_2O (Mt)**	**Ore (Mt)**	**K_2O (%)**	**K_2O (Mt)**	**Ore (Mt)**	**K_2O (%)**	**K_2O (Mt)**	**Ore (Mt)**	**K_2O (%)**	**K_2O (Mt)**
Berezniki 2	7.7	33.7	2.6	33.5	22.7	7.6	253.4	24.3	61.7	-	-	-	294.6	24.4	71.9
Berezniki 4	331.8	21.6	71.5	431.8	22.6	97.4	1,015.0	20.6	209.3	310.3	26.8	83.3	1,778.6	21.3	378.2
Ust-Yayvinsky	169.9	19.0	32.3	311.0	19.8	61.7	809.7	19.8	160.4	-	-	-	1,290.6	19.7	254.4
Solikamsk 1	115.6	17.8	20.6	14.7	15.4	2.2	86.0	16.3	14.0	-	-	-	216.3	17.0	36.8
Solikamsk 2	127.8	19.3	24.7	82.6	13.9	11.5	275.3	18.6	51.2	-	-	-	485.7	18.0	87.4
Solikamsk 3	103.8	17.5	18.1	64.6	18.9	12.2	1,239.6	17.4	216.0	-	-	-	1,408.0	17.5	246.3
Polovodovsky	-	-	-	694.1	16.7	1,15.8	2,386.6	17.4	415.2	260.8	15.3	39.8	3,080.7	17.2	531.0
Total	**857**	**20**	**170**	**1,632**	**19**	**308**	**6,066**	**18.5**	**1,128**	**571**	**21.5**	**123**	**8,555**	**19**	**1,606**

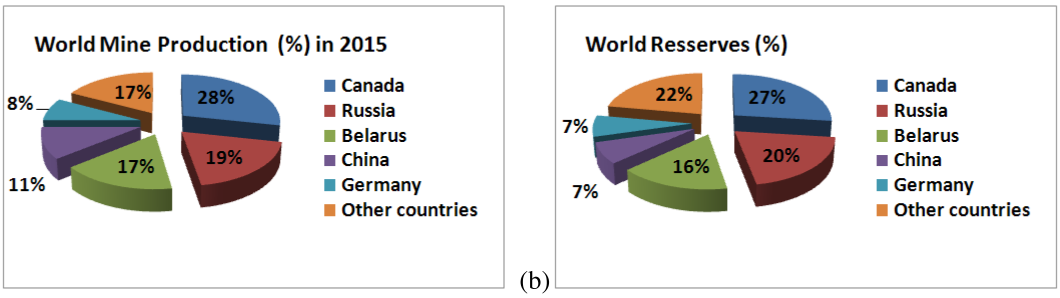

(a) (b)

Figure 2 : (a) Annual production (in %) and (b) global resources in potash (source: [4], [5], [6]).

The USGS currently estimated at 7 billion tons the recoverable global resources of potash[1] [4]. Canadian deposits are huge, thick, with high qualities and relatively easy to exploit, but lying at great depths

[1] About 200 years of estimated resources assuming current consumption.

(Saskatchewan> 900m; New Brunswick> 960m, Canada), and extraction costs tend to increase. 3D modeling can be very useful to estimate the recoverable resources by in-situ leaching and to anticipate future productions. The purpose of this study is to propose a model of the distribution of potash ore bodies, and to infer the areas at risk.

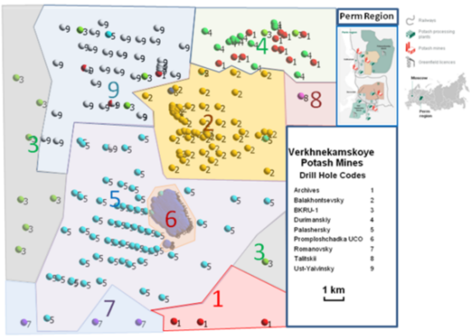

Figure 3. Drill location at Verkhnekamskoye deposit, Russia. Color indicates type of ores.

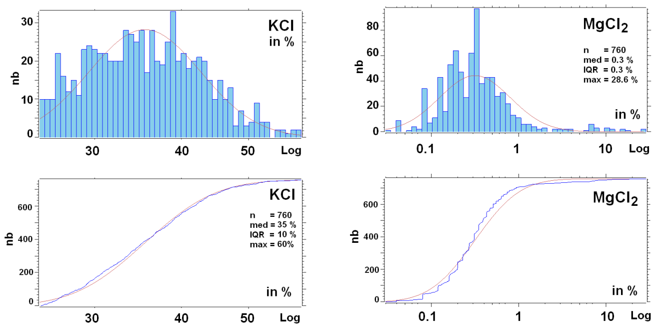

Figure 4. Histograms (top) and cumulative (bottom) distribution of the KCl and $MgCl_2$ grades showing a typical log-normal distribution.

2. Generality on Potash Deposits and available data

Primary potassium resources come from evaporation of sea water (evaporites). Potassium ores are mined from underground deposits, salt lakes and brines. Sylvite (KCl) and halite (NaCl) are the most abundant minerals, mixing the two forms is the ore commonly called sylvinite [7].

2.1. *The Verkhnekamskoye Potash Deposit (Russia)*

Exploited since the early XVth century, the oldest and biggest deposits of potash in the World are located in the Uralkali region (Russia). The ore reserves of the Verkhnekamskoye region potash mines are evaluated at 15.875 Gt (including proved categories (A+B+C_1, a resource classification used in former Russian countries), 56 Gt including the C_2 indicated one, [8]). These huge resources make Russia the third world producer of potash after Canada and Byelorussia. On the 1st January 2015, the total resources in sylvinite (A+B+C_1) of mines exploited by Uralkali (seven in total) were estimated at 4Gt @ 18.8% K_2O (estimated + inferred) presenting 1.388Gt of K_2O.

2.2. *Use of IT techniques in geometallurgy*

Advanced information technology (IT) methods are used for charactering the grade and quality spatial distribution of ores in stratiform deposits. These techniques allow better planning of operations, increased recovery, grade content at production, and better selection of blocks improving the efficiency of flotation. Another advantage of using 3D models is the ability to quantify the strains and stresses using backward restoration techniques [9], and thus ensure a better ground stability during underground operations, and optimization of in-situ leaching. Several dramatic collapses occurred in this mining area of the Verskmanskoy region (in 1986 [1]; in 2007, [10], [11]). These collapses were attributed to the formation of artificial karsts by water inflows intrusion, and had attracted the attention of the security agencies on better mining methods. 3D modelling of the Verkhnekamskoye deposit can help to better understand the geometry of geological structures, their connection with potential aquifers, and to provide the location of faults.

2.3. *Available data for modelling*

The industrial partner provided through the State University of Perm, an Excel™ database of 1,062 drill holes, 7,638 samples and 18 variables (including well number, type, mine, layer, drill, mine, sub-layer, X, Y, roof level, thickness, HO, KCl, $MgCl_2$, NaCl, $CaSO_4$, Comments, Br), used to build a 3D model, and to perform the geostatistical study of the deposit using the 3D gOcad modeller ([12], [13]). A stratigraphic column of the geological formation was reconstructed from borehole data.

3. 3D geomodeling and geostatistics

3.1. 3D modelling

The Excel™ drill holes database was imported in gOcad™ including the coordinates X,Y,Z, the layer label, and grades including KCL, $MgCl_2$, Br, $CaSO_4$, and NaCl. Tops of the A, A', A-A', B. KPI, KPII, and KPIII layers, were fit in the 3D space using a triangulated surface (TSurf)

(a)

(b)

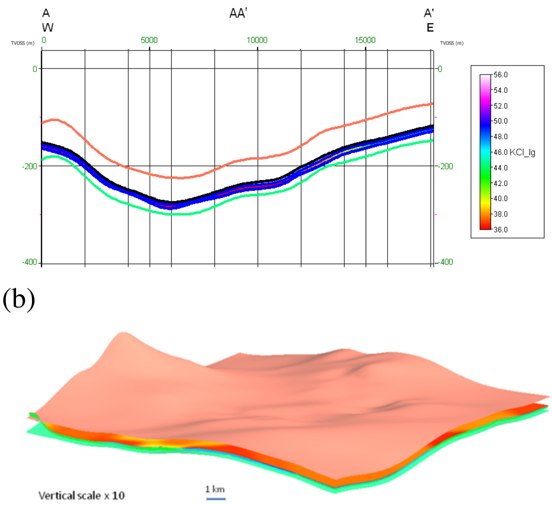

Figure 5. (a) EW Vertical cross-section showing the tops and bases of the A and KPIII mineralized layers; (b) 3D model of the potash mineralized zone. Top surfaces of the mineralized layers A-A', B, KPI, KPII, and KPIII.

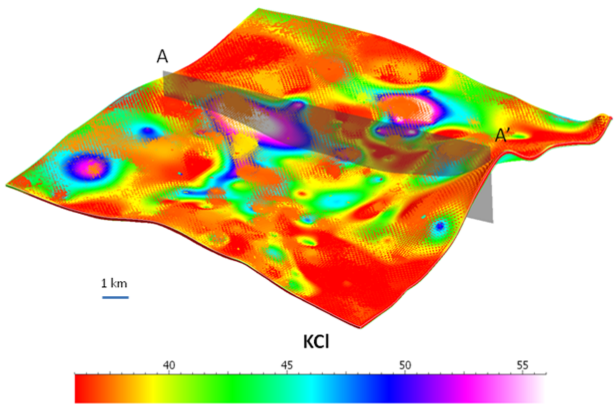

Figure 6. Stratigraphic grid adjusted to the mineralized layers A and KPIII. The color scale indicates the KCl content.

(one per layers) imposing layer thickness, or passing through drills constrains during DSI interpolation. The thicknesses were interpolated using DSI on the top surface for each layer, then used as constrains to re-interpolate the layers, avoiding self-cross-cutting among layers (Figure 5b). A vertical cross-section (Figure 5a) shows the result for layers A and KPIII.

3.2. Statistical study

A study performed on the KCl and $MgCl_2$ grades (mainly on layers A, A', B, KPI, KPII, and KPIII) and on the entire deposit, shows that grades have a classical log-normal distribution. The mean grades in KCl and $MgCl_2$, but also variability, are very high at the Verkhnekamskoye potash deposit, around $36.2_{\pm 6.9}$ %KCl (≈ $22.7_{\pm 4.3}$ %K_2O) and $0.68_{\pm 2.08}$ %$MgCl_2$ (Figure 4). In details, two populations can be identified: (i) a *high* (within 10-50% KCl) grade minable one representing more than 60% concentrated in three homogeneous layers with low variability, and (ii) a *low* (0.1-8% KCl) grades; the same for $MgCl_2$ but with an inverse repartition compared to KCl, the lowest grades (0.01-5% $MgCl_2$) are the most common (70%) while the highest (5-30% $MgCl_2$), the least frequent. This shows that at the beginning of the evaporation cycle, the $MgCl_2$ concentration in the brine was not enough for forming carnallite (KCl, $MgCl_2$ ($6H_2O$)), and sylvinite precipitated while $MgCl_2$ concentrated in the brine. At the end of the cycle, the $MgCl_2$ concentration in the brine was sufficient to form carnallite in small proportions in the upper most layers. Similarly, the gypsite ($CaSO_4$) shows an inverse vertical zoning from top (0.1%) to bottom (2.4 but up to 8%$CaSO_4$), but with only log-normal distribution.

Correlations: Study of correlations between elements shows that they are reproducible from one layer to the others, such as $MgCl_2$ and OH. Thus, the abundance of $MgCl_2$ and OH would indicate the presence of carnallite (KCl, $MgCl_2$ ($6H_2O$)). However, this interpretation must be handled with care as OH can be included in clay minerals or in carbonates[2]. One can estimate the amount of carnallite from $MgCl_2$,

[2] In fact OH is the loss of ignition (L.O.I) and includes all the volatiles elements such as CO_2, F, H_2O, OH, …

and calculate the residual amount of OH. Assuming that this residual corresponds to CO_2 contained in dolomite (CaMg $(CO_3)_2$) (observed in the deposit), one can estimated the average content in dolomite per layer, and observes a vertical increasing amount of dolomite from bottom (KPIII) to top (PT_B), the richest in dolomite [14].

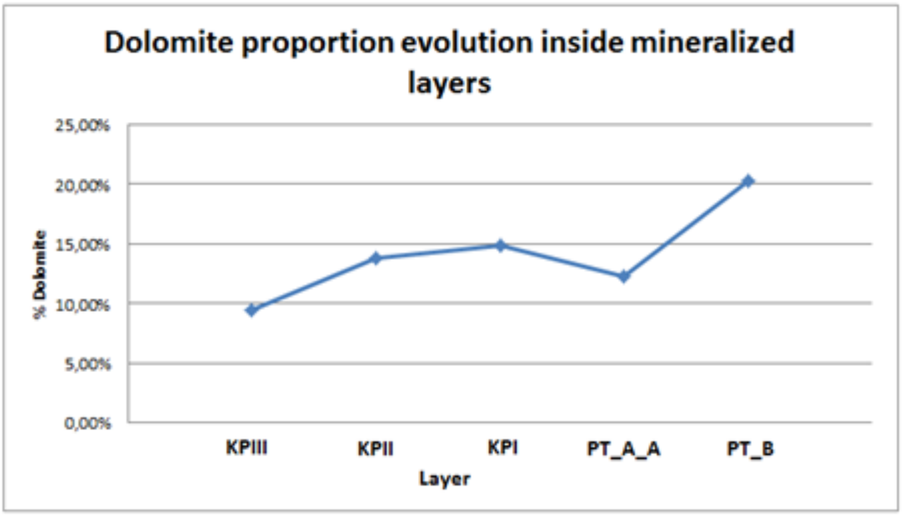

Figure 7. Indirect estimation per layer of the average content in dolomite calculated from the residual amount of OH not included in the carnallite.

3.3. *Spatial variability*

A regular stratigraphic grid (185×194×30 so in total over 1M cells) with elementary cells of about 100×100×2.5m was adjusted on the top and bottom of the mineralized zone in order to calculate the variograms (Figure 6). Variograms were calculated vertically and horizontally along the deformation of the layers (Figure 8a-b). Spatial variations of KCl and $MgCl_2$ point out the existence of an anisotropic structure in the vertical direction with a range of about 20m, and an isotropic structure along the layer with a range of about 1,500m. Variograms were fit to a spherical model with a nugget effect at the origin. Fitted parameters are reported in Figure 8c. They were used to estimate *in-situ* reserves by kriging. This shows that grades can be estimated vertically and horizontally at distances of about 20m and 1,500m, respectively. This spatial structure appears to be valid on the entire deposit and can be used to optimize the sample mesh of the drilling exploration campaign [15].

3.4. *In-situ reserve estimations*

In-situ reserves were estimated by kriging using the drill hole data and the 3D model after interpolating potassium (K) and magnesium (Mg) contents at the nodes of the regular centered stratigraphic grid over one million blocks (or cells). The estimation was then refined on a grid adjusted to the mineralized layers (Figure 9). Total resources in potassium of the mineralized zone vary depending on the cut-off grade. They were estimated between 4.7Gt @ 16.1% K_2O; $MgCl_2$ 0.32% for a cutoff grade exploitation of 13.1% K_2O, and 2.06 Gt @ 18.2% K_2O; $MgCl_2$ 0.32% for a cutoff grade of 16.5% K_2O, respectively. The most important resources are concentrated in the KPI layers KPII and KPIII, the KPI layer being the richest, while the KPIII layer is the largest in terms of tonnage.

4. Defining potential risk map using curvatures

Gaussian (K_G) and mean (K_H) curvatures were calculated on the topography and on each mineralized layer top surface and maps on Figure 11 and Figure 12. They were used to identify lineaments interpreted as possible fractures down cutting at depth the top of the mineralized layers, thus creating flow paths for possible fluid circulations from the surface. These lineaments are mainly oriented along a N30 direction, a regional tectonic direction which can be observed on the topography at a regional scale. These structures seem to continue at depth and can be identified very clearly on the map of curvatures calculated of the top of the KPIII mineralized layer, suggesting that the faults have a more or less vertical dip; no field observations are available to contradict this assumption. These maps were then used to define a risk map of possible collapses areas (Figure 12b).

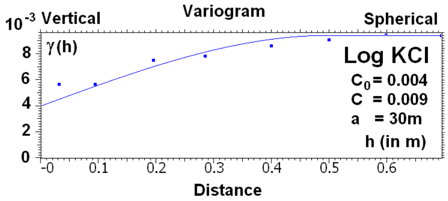

(a)

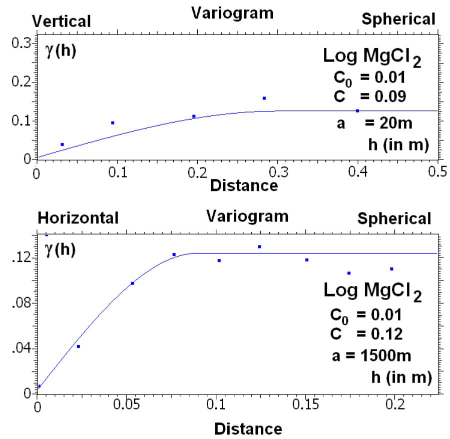

(b)

Region	Element	Variogram type	Range	C	Nugget
Layer 1	KCl	KCl	2 950 m	32	0
	$MgCl_2$	$Log_{10}MgCl_2$	2 300 m	0.44	0
Layer 2	KCl	KCl	2 600 m	14	0
	$MgCl_2$	$Log_{10}MgCl_2$	1 400 m	0.20	0.06
Layer 3	KCl	KCl	2 400 m	25	0
	$MgCl_2$	$Log_{10}MgCl_2$	2 000 m	0.24	0
PT_B	KCl	KCl	2 400 m	0.017	0
PT_A_A	KCl	KCl	0 m	0.019	0.019

(c)

Figure 8. Vertical (a) and horizontal (b) variograms calculated along the geological layers for KCl and $MgCl_2$ showing an anisotropic structure (see text); (c) parameters of the theoretical spherical variogram with nugget effect fitted to the experimental ones for both KCl and $MgCl_2$, and their logarithm.

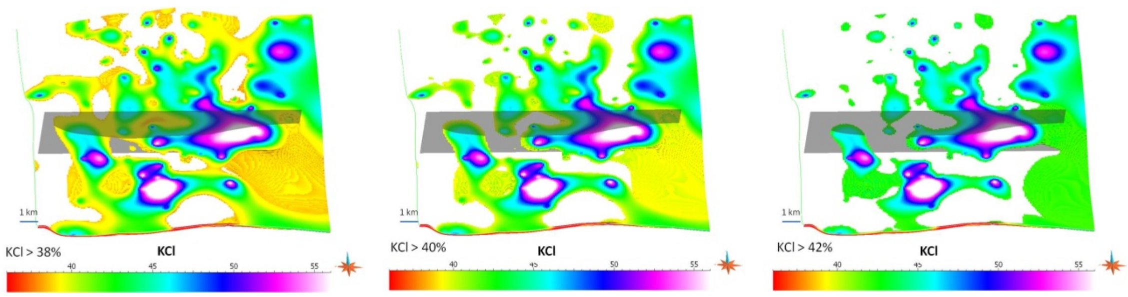

Figure 9. From left to right, mineralized zones defined for different KCl cut-off grades (i.e K_2O> 18.2%, 18.9% and 19.5%).

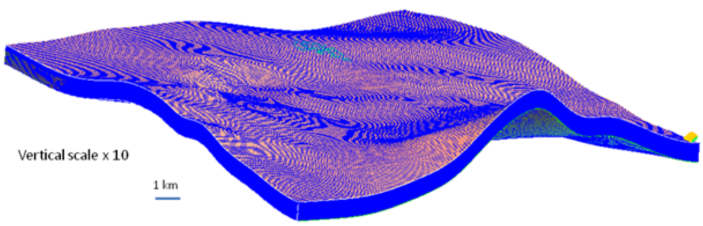

(a) (b)

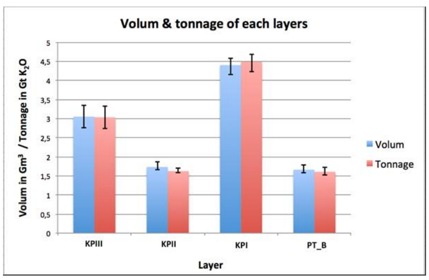

Figure 10. (a) Stratigraphic regular grid using to perform reserves estimation (185×194×30 cells of size 100×100×2.5 m); (b) In-situ volume and ore tonnage estimated per mineralized layer using a sequential Gaussian simulation (SGS) with uncertainty indicated by vertical bars.

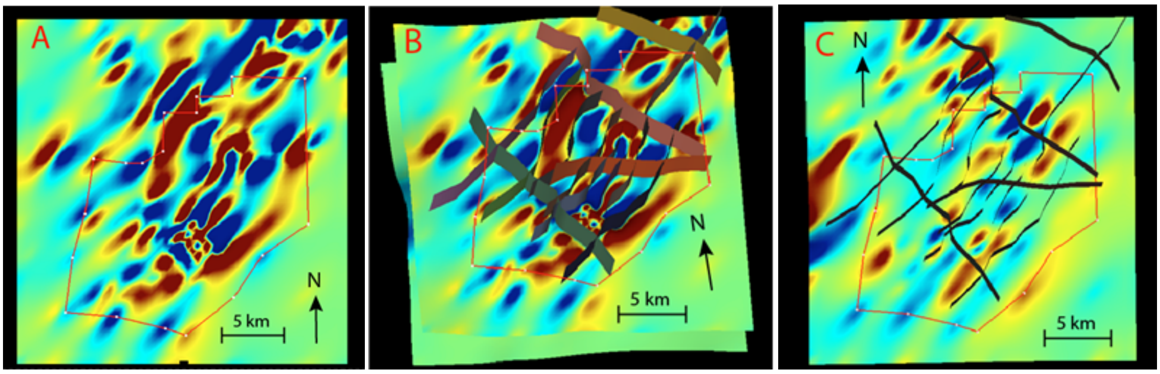

Figure 11. Curvature map calculated on the topography of the Verkhnekamskoye potash deposit (Russia) A: curvature calculated on the topography (without faults); B: same as A with identified faults; C: projection of the faults identified on the topography and extended downward on the mineralized KPIII layer.

(a)
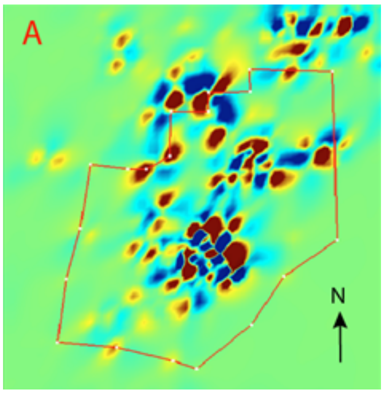

(b)
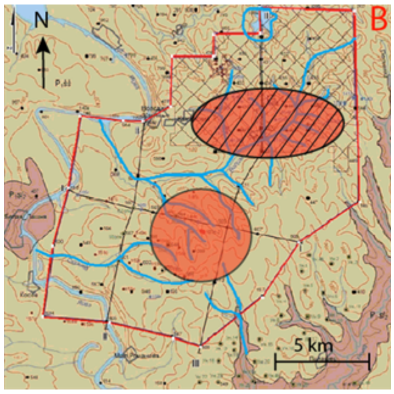

Figure 12. (a). Curvature map calculated on the topography for comparison; (b). Risk map of possible surface collapse areas due to deep dissolution of salt by fluid circulation through faults (in red higher potential risks, hashed smaller risks) superposed on the hydro-geological map with river network (in blue).

5. Conclusions

This work shows important results obtained both on the 3D modelling aspects of the Verkhnekamskoye (Russia) potash deposit, and on the in-situ reserves estimation. The reserve estimation based on the 3D model shows a vertical distribution of KCl and $MgCl_2$ grades compatible with actual knowledge on the formation of evaporites. Total in-situ reserves estimated by kriging vary according to the cut-off between 4.7Gt @ 16.1 % K_2O; 0.32 % $MgCl_2$ for a cut-off grade at 13.1% K_2O and 2.06 Gt @ 18.2 % K_2O; 0.32 % $MgCl_2$ at a cut-off of 16.5% K_2O. Most of reserves are located in the KPI, KPII and KPIII layers, the KPI being the richest, and KPIII the largest in terms of tonnage. Several other aspects were explored, in particular the impact of faulting identified from curvature map, on the hydrogeology system as a risk factor for water intrusion at depth provoking catastrophic dilution of the salt. The most direct consequences of this fault modelling is the defined of high probability risk map of possible collapses areas. As far as we know, this is the first comprehensive 3D model of the Verkhnekamskoye (Russia) potash deposit. However, this is a first attempt which can be further developed for hydro-geological, mechanical and environmental studies.

6. Acknowledgements

The work was supported by the Government of Perm Krai, Russia (grant C-26-004-07).
The authors would like to express their thanks for the support to ASGA and Lorraine-Russia Arcus Project.

References

[1] USGS, Mineral Commodity Summaries and Potash, January 2008.

[2] Potash Corp 2013. Online Annual report, 63p, http://www.potashcorp.com/media/POT_2015_AR_Full_Report.pdf
[3] Uralkali 2013. *Sustainable Leadership*, Intregrated Report & Accounts 2013, 178p.
[4] USGS, Jan 2016, http://minerals.usgs.gov/minerals/pubs/commodity/potash/mcs-2015-potas.pdf
[5] USGS, 2009, http://minerals.usgs.gov/minerals/pubs/commodity/phosphate_rock/mcs-2009-phosp.pdf
[6] USGS, 2017, https://minerals.usgs.gov/minerals/pubs/commodity/potash/mcs-2016-potas.pdf
[7] Garret D 1996. *Potash: Deposits, processing, properties and uses*. Chapman & Hall, London, UK.
[8] Kydryachov A I et al 2006. *Mineral and raw materials inventory of the Perm Region*, Koppektiv abtopov, Perm, 464p.
[9] Moretti I, Lepage F, Guiton M 2006, KINE3D: a new 3D restoration method based on a mixed approach linking geometry and geomechanics. *Oil & Gas Science and Technology, Rev. IFP*, **61**(2), 277-289.
[10] Andrejchuk A 2002. Collapse above the World's largest potash mine (Ural, Russia). *Int. J. Speleol,* **31**(1/4), 137-158.
[11] Ashrafiantar N, Hebel H P and Busch W 2011. *Monitoring of mining induced land subsidence - Differential SAR interferometer and persistent interferometer using TerraSAR-XData in comparison with Envisa Data*. 4th TerraSAR-X Science Team Meeting, 14-16 Feb., DLR, Oberpfaffenhofen, Germany, 7p
[12] gOcad Research Group - http://www.ring-team.org/
[13] Mira Geoscience - http://www.mirageoscience.com/
[14] Litaudon J 2015. *Geostatistic study analysis of the Verkhnekamskoye potash deposit*. Third year project in GeoRessources Laboratory, ENSG Nancy report, France, 27p.
[15] Royer J.J 2013. *Development of Scientific Bases of Mineral Resources High performance flotation & efficiency Improvement of ore enrichment of the K, Mg salts Verkhnekamskoye Deposit.“3D modeling Part”*. 1st Annual Project Report, ENSG, UdL, Nancy, 17p.